Author Manuscript

Author Manuscript

Author Manuscript

Author Manuscript

HHS Public Access

Author manuscript

Nat Med. Author manuscript; available in PMC 2017 January 02.

Published in final edited form as:

Nat Med. 2016 September ; 22(9): 1002–1012. doi:10.1038/nm.4153.

NOX4-dependent fatty acid oxidation promotes NLRP3 inflammasome activation in macrophages

Jong-Seok Moon[1,2], **Kiichi Nakahira**[1,2], **Kuei-Pin Chung**[1,2,3], **Gina M. DeNicola**[1], **Michael Jakun Koo**[1,2], **Maria A. Pabón**[1], **Kristen T. Rooney**[1,2], **Joo-Heon Yoon**[4,5,6], **Stefan W. Ryter**[1,2], **Heather Stout-Delgado**[1,2], and **Augustine M. K. Choi**[1,2,*]

[1]Joan and Sanford I. Weill Department of Medicine, Weill Cornell Medical College and New York-Presbyterian Hospital, New York, USA.

[2]Division of Pulmonary and Critical Care Medicine, Weill Cornell Medical College, New York, NY, USA.

[3]Department of Laboratory Medicine, National Taiwan University Hospital and National Taiwan University Cancer Center, Taipei, Taiwan.

[4]Research Center for Natural Human Defense System, Yonsei University College of Medicine, Seoul, South Korea.

[5]Department of Otorhinolaryngology, Yonsei University College of Medicine, Seoul, South Korea.

[6]The Airway Mucus Institute, Yonsei University College of Medicine, Seoul, South Korea.

Abstract

Metabolic regulation has been implicated in the pathogenesis of inflammatory diseases. NADPH oxidase 4 (NOX4), a source of cellular superoxide anion, has multiple biological functions that may be of importance in inflammation, and in the pathogenesis of human metabolic diseases, including diabetes. However, the mechanisms by which NOX4-dependent metabolic regulation impacts the innate immune response remain unclear. Here, we show that deficiency of NOX4 resulted in reduced expression of carnitine palmitoyltransferase 1A (CPT1A), which is a key mitochondrial enzyme in the fatty acid oxidation (FAO) pathway. The reduced FAO resulted in less activation of the nucleotide binding domain, leucine-rich repeat-containing receptor (NLR), pyrin domain-containing-3 (NLRP3) inflammasome in human and mouse macrophages. In contrast, NOX4 deficiency did not inhibit the activation of the NLR family, CARD domain

*Correspondence to: amc2056@med.cornell.edu (A.M.K.C).

AUTHOR CONTRIBUTIONS

J.-S.M, K.N. and A.M.K.C conceived of the study with assistance from S.W.R.; J.-S.M., K.-P.C., G.M.D., M.J.K., M.A.P. and K.T.R. contributed the *in vitro* experiments; J.-S.M. and H.S.-D. contributed the *in vivo* experiments; J.-S.M. contributed all *in vitro* and *in vivo* experiments; K.-P.C. contributed the experiments for ASC oligomerization and ASC speck formation; M.A.P. contributed the experiments for human subjects; G.M.D. contributed the experiments for FAO assay; M.J.K. and K.T.R. contributed the experiments for cytokine analysis; J.-S.M., J.-H.Y., K.N., S.W.R. and A.M.K.C. wrote the paper; and A.M.K.C supervised the entire project.

COMPETING FINANCIAL INTERESTS

The authors declare no competing financial interests.

Health sciences/Diseases/Infectious diseases/Bacterial infection
Biological sciences/Biochemistry/Lipids/Fatty acids
Biological sciences/Immunology/Inflammation/Inflammasome
Health sciences/Diseases/Respiratory tract diseases

Author Manuscript Author Manuscript Author Manuscript Author Manuscript

containing 4 (NLRC4), the NLRP1, or the absent in melanoma 2 (AIM2) inflammasomes. We also found that inhibition of FAO by etomoxir suppressed NLRP3 inflammasome activation. Furthermore, *Nox4*-deficient mice displayed significant reduction of caspase-1 activation and interleukin (IL)-1β and IL-18 production and improved survival in a mouse model of NLRP3-mediated *Streptococcus pneumoniae* (*S. pneumoniae*) infection. The pharmacologic inhibition of NOX4 by either GKT137831, currently in phase 2 clinical trials, or VAS-2870 attenuated NLRP3 inflammasome activation. Our results suggest that NOX4-mediated FAO promotes NLRP3 inflammasome activation.

The NLRP3 inflammasome, a molecular platform that modulates innate immune functions by activation of caspase-1, catalyzes the proteolytic processing and secretion of IL-1β and IL-18 in immune cells[1,2]. Cellular metabolites have been linked to NLRP3 inflammasome activation[3–5]. We have previously reported that cellular metabolic pathways, including glycolysis and fatty acid synthesis, are associated with NLRP3 inflammasome activation in macrophages under pro-inflammatory conditions[6,7]. Notably, fatty acid metabolism has been linked to NLRP3 inflammasome activation[4,5,7] ,a process that is implicated in metabolic diseases such as obesity-derived diabetes or insulin resistance[8]. As a mechanism for the utilization of fatty acids, FAO is a major bioenergetic pathway, which is upregulated under conditions of prolonged fasting, exercise or metabolic stress[9,10]. Among the enzymes in the FAO pathway, the reduced activity of CPT1A, which is essential for the proper transport and oxidation of long chain fatty acids (LCFAs) in mitochondria may promote type 2 diabetes and insulin resistance[11,12]. Recently, mitochondrial NOX4 has been implicated in oxidative stress and mitochondrial function in the diabetic kidney and heart[13–21]. Currently, the role of NOX4 in regulating cellular metabolism during NLRP3 inflammasome activation remains incompletely understood. In this study we sought to identify the mechanisms by which NOX4 regulates the NLRP3 inflammasome, which is a key mediator of macrophage-dependent inflammation through regulation of mitochondria-dependent metabolic pathways.

RESULTS

Deficiency of NOX4 suppresses NLRP3 inflammasome activation

To investigate the function of NOX4 in NLRP3 inflammasome activation, we analyzed whether genetic deficiency of NOX4 could suppress the secretion of IL-1β and IL-18 in lipopolysaccharide (LPS)-primed bone marrow-derived macrophages (BMDMs) in response to specific NLRP3 inflammasome activators, including nigericin, ATP and silica. *Nox4*$^{-/-}$ BMDMs displayed significantly lower IL-1β and IL-18 secretion (Fig. 1a) in response to nigericin, ATP and silica compared to wild-type (WT) BMDMs, while tumor necrosis factor (TNF)-α was unchanged (Fig. 1a). In contrast, deficiency of NOX4 had no effect on the secretion of IL-1β and IL-18 in response to muramyldipeptide (MDP), a NLRP1 inflammasome activator, or flagellin, a NLRC4 inflammasome activator (Fig. 1a). IL-1β secretion was not changed in *Nox4*$^{-/-}$ BMDMs treated with poly(dA:dT), an AIM2 inflammasome activator, relative to WT BMDMs (Fig. 1b). Notably, *Nox4*$^{-/-}$ BMDMs displayed lower expression of cleaved caspase-1 and cleaved IL-1β in response to nigericin and ATP, relative to WT BMDMs, while pro-IL-1β expression was unchanged (Fig. 1c and Supplementary Fig. 1a).

Author Manuscript Author Manuscript Author Manuscript Author Manuscript

Furthermore, we also investigated the role of NOX4 in NLRP3 inflammasome activation in human cells. Thus, to examine whether genetic deficiency of *NOX4* could suppress caspase-1 activation, we used two independent *NOX4*-targeted gRNAs to delete human *NOX4* in primary human macrophages *via* CRISPR technology and found that the activation of caspase-1 and IL-1β cleavage in response to LPS and nigericin were lower compared to transduction with the control plasmid (Fig. 1d). Consistently, the secretion of IL-1β and IL-18 in response to nigericin and ATP were significantly lower when cells were transduced with the two *NOX4*-targeted gRNAs relative to the control plasmid (Fig. 1e), while TNF-α was unchanged (Supplementary Fig. 1b). Next, we investigated the role of NOX4 in a mouse model of *S. pneumoniae* lung-infection. *S. pneumoniae*, a leading cause of pneumonia and meningitis, activates the NLRP3 inflammasome through its secreted pore-forming toxin pneumolysin[22,23]. The levels of IL-1β, IL-18 and TNF-α (Fig. 1f), NOX4 protein expression, and caspase-1 activation (Fig. 1g) in lung tissues of WT mice were higher after *S. pneumoniae* infection relative to vehicle-treated mice. Notably, the levels of IL-1β and IL-18 (Fig. 1f) and caspase-1 activation (Fig. 1g) in lung tissues were significantly lower in *S. pneumoniae*-infected *Nox4*$^{-/-}$ mice compared to infected WT mice, whereas TNF-α was comparable (Fig. 1f). Moreover, *Nox4*$^{-/-}$ mice were more resistant to *S. pneumoniae*-induced mortality at 150 h post-infection than WT mice (Fig. 1h). Furthermore, the plasma levels of IL-1β and IL-18 in response to LPS challenge *in vivo* was significantly lower in *Nox4*$^{-/-}$ mice compared to WT mice, whereas TNF-α was unchanged (Supplementary Fig. 1c). These results suggest that NOX4 regulates NLRP3 inflammasome activation *in vitro* and *in vivo*.

NOX4 regulates FAO during NLRP3 inflammasome activation

We next investigated the underlying molecular mechanism by which NOX4 regulates NLRP3 inflammasome activation. Among the six isoform genes of *Nox* tested (*Nox*1–4 and dual oxidase (*Duox*)1–2), we identified that *Nox4* gene expression was higher in response to ATP in LPS-primed WT BMDMs, relative to BMDMs treated with LPS alone or ATP alone or untreated BMDMs, while the expression of the other *Nox* isoform genes were not specifically regulated by LPS and ATP stimulation (Supplementary Fig. 1d). Furthermore, we found that NOX4 protein was preferentially expressed in mitochondria and its expression was markedly higher in response to nigericin and ATP stimulation in LPS-primed WT BMDMs, relative to LPS alone, or control (Fig. 2a). Moreover, NOX4 protein expression was increased in response to nigericin and ATP in a time and dose-dependent manner in LPS-primed WT BMDMs (Supplementary Fig. 1e,f), while LPS alone did not induce NOX4 expression (Supplementary Fig. 1g). Consistently, treatment with silica and MSU, as well as *A. hydrophila aerolysin*, representative of particulate and bacterial toxin inducers of NLRP3, respectively, resulted in higher NOX4 protein expression and IL-1β secretion in LPS-primed WT BMDMs (Supplementary Fig. 1h,i).

Next, we examined whether NOX4-derived reactive oxygen species (ROS) could regulate cellular metabolism during NLRP3 inflammasome activation. *Nox4*$^{-/-}$ BMDMs had significantly lower mitochondrial ROS (mtROS) production in response to LPS and nigericin relative to WT BMDMs (Fig. 2b). As ROS is associated with FAO in myoblasts[24], we analyzed the regulation of FAO by NOX4 during NLRP3 inflammasome activation. We

Author Manuscript Author Manuscript Author Manuscript Author Manuscript

observed that the uptake of free fatty acids (FFAs) including LCFAs and poly-unsaturated fatty acids (PUFAs), were significantly higher in response to LPS and ATP in WT BMDMs, relative to LPS alone, or control (Supplementary Fig. 2a). FFAs levels were significantly lower in *Nox4*$^{-/-}$ BMDMs in response to LPS and nigericin relative to WT BMDMs (Fig. 2c). Consistently, the protein expression of LCFA transporter cluster of differentiation 36 (CD36), which facilitates the cellular uptake of LCFAs such as palmitate and stearate[25], was lower in *Nox4*$^{-/-}$ BMDMs in response to LPS and nigericin compared to WT BMDMs (Supplementary Fig. 2b).

As FFAs are broken down and utilized by FAO for release of energy[9], we evaluated whether NOX4 could regulate FAO during NLRP3 inflammasome activation. We measured the oxidation of fatty acids by monitoring cellular oxygen consumption rate (OCR) with palmitate-BSA treatment, as an FAO substrate[9,26]. The OCR was higher in response to nigericin stimulation in LPS-primed WT BMDMs compared to LPS alone or untreated control and this relative response to LPS and nigericin was higher in response to palmitate-BSA treatment (Fig. 2d and Supplementary Fig. 2c). *Nox4*$^{-/-}$ BMDMs had lower OCR in response to palmitate-BSA compared to WT BMDMs after LPS and nigericin treatments (Fig. 2d and Supplementary Fig. 2c). In contrast to *Nox4*$^{-/-}$ BMDMs, the activation of FAO by palmitate-BSA resulted in higher caspase-1 activation, IL-1β cleavage (Fig. 2e and Supplementary Fig. 2d) and secretion of IL-1β and IL-18 (Fig. 2f) in response to nigericin and ATP in LPS-primed WT BMDMs relative to control, whereas TNF-α was unchanged in both WT and mutant BMDMs (Fig. 2f). Similar to palmitate-BSA, stearic acid-BSA treatment, one of the most common saturated fatty acids[27], resulted in higher caspase-1 activation, IL-1β cleavage (Supplementary Fig. 2e,f) and secretion of IL-1β and IL-18 (Supplementary Fig. 2g) in response to nigericin and ATP relative to control, while TNF-α was unchanged (Supplementary Fig. 2g). *Nox4*$^{-/-}$ BMDMs had lower caspase-1 activation, IL-1β cleavage (Supplementary Fig. 2e,f) and secretion of IL-1β and IL-18 (Supplementary Fig. 2g) in response to stearic acid-BSA than WT BMDMs.

As the oxidation of FAs by FAO generates acetyl-CoA, which fuels the tricarboxylic acid cycle (TCA) cycle[8,9], the levels of acetyl-CoA were higher in response to either nigericin or palmitate-BSA and nigericin in WT BMDMs, relative to *Nox4*$^{-/-}$ BMDMs (Fig. 2g). Since the ECAR, as an index of glycolytic rate, was comparable between WT and *Nox4*$^{-/-}$ BMDMs, lower acetyl-CoA production in *Nox4*$^{-/-}$ BMDMs was not affected by glycolysis (Supplementary Fig. 2h). In contrast, the protein expression of glucose-6-phosphate dehydrogenase (G6PD), the rate-limiting enzyme of the pentose phosphate pathway[28], was comparable between WT and *Nox4*$^{-/-}$ BMDMs in response to LPS and nigericin stimulation (Supplementary Fig. 2i).

Next, we investigated whether NOX4-dependent FAO could regulate the oligomerization of the adaptor apoptosis-associated speck-like protein containing a caspase recruitment domain (ASC), which is required for NLRP3-dependent caspase-1 activation[29,30]. The formation of ASC monomers and higher complexes (Fig. 2h) and speck formation (Fig. 2h) induced by LPS and nigericin stimulation was greater in WT BMDMs than in *Nox4*$^{-/-}$ BMDMs. Furthermore, NOX4 overexpression resulted in higher levels of FFA and acetyl-CoA in response to nigericin in LPS-primed WT peritoneal macrophages compared to control (Fig.

Author Manuscript Author Manuscript Author Manuscript Author Manuscript

2i). Moreover, NOX4 overexpression resulted in higher caspase-1 activation, IL-1β cleavage (Fig. 2j) and secretion of IL-1β and IL-18 (Fig. 2j) in response to LPS and nigericin relative to control, while TNF-α was unchanged (Fig. 2j). In the absence of LPS priming, NLRP3 overexpression supported caspase-1 activation in response to nigericin or ATP (Supplementary Fig. 3a), and this effect was lower in *Nox4*$^{-/-}$ BMDMs compared to WT BMDMs (Supplementary Fig. 3b). These results suggest that NOX4 regulates FAO during NLRP3 inflammasome activation.

NOX4 regulates CPT1A during NLRP3 inflammasome activation

We next investigated the targets of NOX4 in the regulation of FAO during NLRP3 inflammasome activation. Notably, *Nox4*$^{-/-}$ BMDMs displayed lower protein expression of CPT1A, which is a key enzyme for mitochondrial FAO[31], in response to LPS and nigericin relative to WT BMDMs (Fig. 3a), while the protein expression of CPT1C and acyl-coenzyme A oxidase 1 (ACOX1), which is a key enzyme of peroxisomal FAO[32], were comparable (Fig. 3a). Since K^+ efflux is increased by specific NLRP3 inflammasome activators[33], we investigated whether K^+ efflux could regulate NOX4 and CPT1A expression during NLRP3 inflammasome activation. First, we analyzed the regulation of NOX4 by K^+ efflux. The gene expression levels of *Nox4* in response to nigericin were significantly lower in the presence of high extracellular [K^+] in LPS-primed WT BMDMs compared to control (Fig. 3b). Consistently, the induction of NOX4 and CPT1A protein expression, caspase-1 activation, IL-1β cleavage and the secretion of IL-1β (Fig. 3c and Supplementary Fig. 3c) in response to nigericin were lower in the presence of high extracellular [K^+] in LPS-primed WT BMDMs relative to control, while TNF-α was unchanged (Supplementary Fig. 3c). Similarly, treatment with glyburide, an inhibitor of ATP-sensitive K^+ (K_{ATP}) channels[34], resulted in lower protein expression of NOX4 and CPT1A, caspase-1 activation, IL-1β cleavage (Supplementary Fig. 3d) and secretion of IL-1β (Supplementary Fig. 3e) in response to nigericin relative to control, while TNF-α was unchanged (Supplementary Fig. 3e). In contrast, the higher expression of NOX4 and CPT1A in response to LPS and nigericin were not altered in *Nlrp3*$^{-/-}$ BMDMs compared to WT BMDMs (Supplementary Fig. 3f).

To investigate the molecular mechanism by which NOX4 regulates the expression of CPT1A, we analyzed the role of NOX4-derived mtROS in regulating CPT1A expression during NLRP3 inflammasome activation. Treatment with Mito-TEMPO, a specific scavenger of mitochondrial superoxide[35], resulted in lower protein expression of CPT1A, caspase-1 activation and IL-1β cleavage in response to nigericin in LPS-primed WT BMDMs compared to control (Fig. 3d). Consistently, Mito-TEMPO treatment resulted in significantly lower induction of OCR by palmitate-BSA (Fig. 3e and Supplementary Fig. 3g) and levels of FFA (Fig. 3f) in response to nigericin compared to control. In contrast, the protein expression of PPAR-γ coactivator-1α (PGC-1α), which is a key transcription factor that regulates the expression of proteins involved in fatty acid uptake and oxidation[36], was comparable between *Nox4*$^{-/-}$ and WT BMDMs (Supplementary Fig. 3h). Consistently, the gene expression of *Cpt1a* was not changed in response to LPS and nigericin in *Nox4*$^{-/-}$ BMDMs compared to WT BMDMs (Supplementary Fig. 3i). These results suggest that NOX4-derived mtROS is critical for the regulation of CPT1A protein expression.

Author Manuscript Author Manuscript Author Manuscript Author Manuscript

Inhibition of FAO suppresses NLRP3 inflammasome activation

To examine whether genetic deficiency of *Cpt1a* could suppress caspase-1 activation, we used two independent *Cpt1a*-targeted gRNAs against mouse *Cpt1a* and CRISPR technology in WT BMDMs. Transduction with *Cpt1a*-targeted gRNAs resulted in a lower degree of activation of caspase-1, IL-1β cleavage (Fig. 4a), and secretion of IL-1β and IL-18 (Fig. 4b) in response to nigericin and ATP compared to the control plasmid, while TNF-α was unchanged (Fig. 4b). Similarly, the activation of caspase-1, cleaved IL-1β (Supplementary Fig. 4a), and the secretion of IL-1β and IL-18 (Supplementary Fig. 4b) in response to nigericin and ATP were lower in response to two independent *Cpt1a* shRNAs against mouse *Cpt1a* relative to control shRNA in WT peritoneal macrophages, while TNF-α was unchanged (Supplementary Fig. 4b). Moreover, the production of acetyl-CoA in response to nigericin and ATP were lower after transduction with two independent *Cpt1a* shRNAs compared to control shRNA (Supplementary Fig. 4c). Consistently, palmitate-BSA-induced activation of caspase-1, cleaved IL-1β (Supplementary Fig. 4d) and the secretion of IL-1β and IL-18 (Supplementary Fig. 4e) in response to nigericin and ATP were lower after transduction with *Cpt1a* shRNA, while TNF-α was unchanged (Supplementary Fig. 4e). NLRP3-dependent ASC oligomerization in response to LPS and nigericin was lower after transduction with a *Cpt1a*-targeted gRNA relative to the control plasmid (Fig. 4c). Furthermore, CPT1A overexpression resulted in higher caspase-1 activation, IL-1β cleavage (Supplementary Fig. 5a) and secretion of IL-1β and IL-18 (Supplementary Fig. 5b) in response to nigericin in LPS-primed BMDMs relative to control, while TNF-α was unchanged (Supplementary Fig. 5b). The inhibition of caspase-1 activation, IL-1β cleavage (Fig. 4d) and secretion of IL-1β and IL-18 (Fig. 4e) were reversed by overexpression of CPT1A in *Nox4*$^{-/-}$ BMDMs compared to control, while TNF-α was unchanged (Fig. 4e).

Moreover, treatment with etomoxir, a specific inhibitor of CPT1[37], resulted in significantly less secretion of IL-1β and IL-18 in response to nigericin, ATP and silica in LPS-primed WT BMDMs compared to vehicle control (Supplementary Fig. 5c), while TNF-α was unchanged (Supplementary Fig. 5c). In contrast, the secretion of IL-1β and IL-18 by MDP, flagellin or poly(dA:dT) stimulation was unchanged by etomoxir (Supplementary Fig. 5c). Consistently, the activation of caspase-1 and IL-1β cleavage in response to nigericin and ATP was lower in response to etomoxir relative to vehicle control (Supplementary Fig. 5d). Similar with *Cpt1a* knockdown, etomoxir treatment resulted in lower palmitate-BSA-induced activation of caspase-1, cleaved IL-1β (Fig. 4f) and secretion of IL-1β and IL-18 (Fig. 4g) in response to nigericin and ATP compared to vehicle control, while TNF-α was unchanged (Fig. 4g). These results suggest that FAO is required for NLRP3 inflammasome activation in response to pro-inflammatory stimuli.

Pharmacological targeting of NLRP3 inflammasome activation

We examined the effects of pharmacologic inhibition of NOX4 on NLRP3 inflammasome activation. Inhibition of NOX4 activity by GKT137831, a potent dual NOX1/4 inhibitor, currently in phase 2 trials[38], resulted in significantly lower secretion of IL-1β and IL-18 in response to nigericin, ATP and silica in LPS-primed peritoneal macrophages compared to vehicle control (Fig. 5a), while TNF-α was unchanged (Fig. 5a). GKT137831 dose-dependently lowered IL-1β secretion in response to nigericin relative to vehicle control,

Author Manuscript Author Manuscript Author Manuscript Author Manuscript

while TNF-α was unchanged (Fig. 5b). Moreover, GKT137831 treatment resulted in lower activation of caspase-1 and cleaved IL-1β (Supplementary Fig. 6a) and secretion of IL-1β and IL-18 (Supplementary Fig. 6b) in LPS-primed WT BMDMs in response to nigericin and ATP compared to vehicle control, while TNF-α was unchanged (Supplementary Fig. 6b). In contrast, the secretion of IL-1β and IL-18 by MDP or flagellin stimulation was unchanged by GKT137831 (Fig. 5a). GKT137831 treatment resulted in significantly lower mtROS production (Fig. 5c and Supplementary Fig. 6c), CPT1A protein expression (Fig. 5d), induction of OCR by palmitate-BSA (Fig. 5e and Supplementary Fig. 6d) and levels of FFA and acetyl-CoA (Fig. 5f and Supplementary Fig. 6e) in response to nigericin relative to vehicle control. Furthermore, GKT137831 treatment resulted in lower palmitate-BSA-induced activation of caspase-1, cleaved IL-1β (Supplementary Fig. 6f) and secretion of IL-1β and IL-18 (Fig. 5g) in response to nigericin compared to vehicle control, while TNF-α was unchanged (Fig. 5g). GKT137831 treatment resulted in significantly lower plasma levels of IL-1β and IL-18 in response to LPS challenge *in vivo* in WT mice relative to vehicle control, whereas TNF-α was unchanged (Supplementary Fig. 6g). Notably, GKT137831 prophylactically lowered the levels of IL-1β and IL-18 (Fig. 5h) and caspase-1 activation (Supplementary Fig. 6h) by *S. pneumoniae* infection in WT lung tissues compared to vehicle control, while TNF-α was comparable (Fig. 5h). These results suggest that GKT137831 reduces NLRP3 inflammasome activation *in vitro* and *in vivo*.

As GKT137831 has dual specificity for NOX1/4[38], we examined the effects of either NOX4 or NOX1 inhibition on NLRP3 inflammasome activation. VAS-2870, a specific NOX4 inhibitor[10], significantly lowered IL-1β secretion in response to nigericin, ATP and silica in LPS-primed WT peritoneal macrophages, compared to vehicle control (Supplementary Fig. 7a). In contrast, VAS-2870 had no effect on the secretion of IL-1β in response to MDP, flagellin or poly(dA:dT) compared to vehicle control (Supplementary Fig. 7a). VAS-2870 treatment resulted in lower caspase-1 activation, IL-1β cleavage (Supplementary Fig. 7b) and secretion of IL-1β and IL-18 (Supplementary Fig. 7c) in LPS-primed WT BMDMs in response to nigericin and ATP relative to vehicle control, while TNF-α was unchanged (Supplementary Fig. 7c). Moreover, VAS-2870 treatment resulted in lower mtROS production (Fig. 6a and Supplementary Fig. 7d), CPT1A protein expression (Fig. 6b), induction of OCR by palmitate-BSA (Fig. 6c and Supplementary Fig. 7e), levels of FFA and acetyl-CoA (Fig. 6d and Supplementary Fig. 7f) in response to nigericin relative to vehicle control in LPS-primed WT BMDMs. Consistently, VAS-2870 treatment lowered palmitate-BSA-induced caspase-1 activation, IL-1β cleavage (Supplementary Fig. 7g) and secretion of IL-1β and IL-18 (Fig. 6e) in response to nigericin compared to vehicle control, while TNF-α was unchanged (Fig. 6e).

In contrast, inhibition of NOX1 activity by ML171, a specific NOX1 inhibitor[10], did not affect caspase-1 activation (Supplementary Fig. 8a) and secretion of IL-1β, IL-18 and TNF-α in LPS-primed WT peritoneal macrophages in response to nigericin and ATP (Supplementary Fig. 8b,c) compared to control. Notably, GKT137831 and VAS-2870 resulted in lower caspase-1 activation, IL-1β cleavage (Fig. 6f,g) and the secretion of IL-1β and IL-18 (Fig. 6h) in response to nigericin and ATP relative to vehicle control in LPS-primed primary human macrophages, while TNF-α was unchanged (Supplementary Fig. 8d). Similar to GKT137831, VAS-2870 treatment significantly lowered plasma levels of

Author Manuscript Author Manuscript Author Manuscript Author Manuscript

IL-1β and IL-18 in response to LPS challenge *in vivo* in WT mice compared to vehicle control, whereas TNF-α was unchanged (Supplementary Fig. 8e).

Moreover, VAS-2870 prophylactically lowered the levels of IL-1β and IL-18 during *S. pneumoniae* infection in WT lung tissues compared to vehicle control (Fig. 6i), while TNF-α was comparable (Fig. 6i). Furthermore, we examined the therapeutic effects of VAS-2870 on the survival of WT mice after *S. pneumoniae* infection (Supplementary Fig. 8f). As the expression of IL-1β is significantly higher at 6 h in *S. pneumoniae*-infected WT BMDMs relative to uninfected BMDMs[18], we treated WT mice therapeutically with VAS-2870 12 h after *S. pneumoniae* infection (Supplementary Fig. 8f). VAS-2870 treatment increased the survival of WT mice after *S. pneumoniae* infection at 150 h post-infection compared to vehicle control (Supplementary Fig. 8f). In contrast, VAS-2870 did not change the levels of IL-1β, IL-18 and TNF-α by *S. pneumoniae* infection in *Nox4*$^{-/-}$lung tissues relative to WT lung tissues (Supplementary Fig. 8g). These results suggest that NOX4 is the pharmacologic target in the pathogenesis of *S. pneumoniae*.

DISCUSSION

Obesity-induced metabolic diseases, such as insulin resistance or type 2 diabetes, are linked to inflammasome activation[8]. High-fat diet (HFD)-derived fatty acids are important contributors to type 2 diabetes[39,40]. Recent studies suggest that HFD or FFAs induce NLRP3 inflammasome activation in adipose tissues and macrophages[4,8,41]. Although the role of fatty acids in NLRP3 inflammasome activation has been demonstrated, the molecular targets that trigger oxidation or utilization of fatty acids during NLRP3 inflammasome activation are not well understood. Our findings provide a molecular mechanism by which NOX4-dependent activation of FAO *via* CPT1A is critical for NLRP3 inflammasome activation by stimuli such as ATP and nigericin. Consistent with our findings, overload of FFAs, such as palmitate, increases NLRP3 inflammasome activation[4]. Of note, this previous study indicates that inhibition of AMP-activated protein kinase (AMPK) can promote NLRP3 inflammasome activation by LPS and FFAs such as palmitate, but not by NLRP3 inflammasome activators used in our study such as ATP and nigericin[4]. Consistently, our previous study showed that the function of AMPK is not changed during NLRP3 inflammasome activation by LPS and ATP[6]. Since AMPK serves as one of the central regulators of cellular energy metabolism[42], AMPK may modulate FAO and other metabolic pathways associated with NLRP3 inflammasome activation, though its role in the NOX4-dependent inflammasome regulation remains unclear at present.

In this report, we demonstrate that NOX4-dependent regulation of FAO promotes the activation of the NLRP3 inflammasome. We also demonstrate that FAO *via* CPT1A is required for NLRP3 inflammasome activation. Furthermore, we show that genetic and pharmacologic inhibition of NOX4 suppresses NLRP3 inflammasome activation in primary human macrophages. Fatty acid metabolism differentially regulates both the priming and activation steps associated with NLRP3 inflammasome regulation in response to pro-inflammatory stimuli[4,5,7]. We have previously reported that fatty acid synthesis is required for the priming step in NLRP3 inflammasome regulation[7]. Here, we have demonstrated that

Author Manuscript Author Manuscript Author Manuscript Author Manuscript

NOX4-dependent FAO is required for NLRP3-dependent ASC oligomerization and speck formation during NLRP3 inflammasome activation.

FAO is essential for energy homeostasis and is mainly regulated by mitochondrial FAO *via* CPT1[43]. The metabolic function of CPT1 is involved in the regulation of insulin secretion in pancreatic β-cells[44,45]. Similarly, the high FFAs levels of plasma are linked to insulin resistance[46,47]. Consistent with these previous studies, the mitochondrial NOX4 is up-regulated in diabetes[16]. Our results indicate that CPT1A–mediated FAO could be a potential pharmacologic target of NOX4 in cellular metabolic pathways. Consistent with previous studies[4,48–50], our results suggest that NOX4-dependent FAO activation might be a metabolic pathway for inflammasome regulation related to the dysfunction of insulin signaling.

Although potential small molecule inhibitors (*e.g.*, β-hydroxybutyrate, MCC950) of the NLRP3 inflammasome have been identified[5,51], further work will be needed to identify their precise mechanisms of action in advance of their clinical development. Here, we describe a mechanism whereby NOX4-dependent CPT1A activation promotes NLRP3 inflammasome activation. Our findings suggest that NOX4 and CPT1A may represent molecular targets of therapeutic inhibitors of the NLRP3 inflammasome. Since our results demonstrate the potential of the NOX1/4 inhibitor GKT137831, currently already in phase 2 human clinical trials, as an NLRP3 inflammasome inhibitor, we anticipate the GKT137831 inhibitor to be more appealing for use in inflammatory metabolic human diseases in the future. Furthermore, our results also indicate that NOX4 may represent a pharmacologic target in the treatment of pneumonia.

In conclusion, these findings demonstrate that the metabolic function of NOX4 could be a therapeutic target in metabolic diseases where NLRP3-mediated inflammation is implicated in the pathogenesis.

ONLINE METHODS

General experimental approaches

No samples, mice or data points were excluded from the reported analyses. Samples were not randomized to experimental groups. Mouse experiments and analyses were not performed in a blinded fashion.

Mice

The *Nox4*$^{-/-}$ mice were from Jackson laboratory. C57BL/6 and *Nox4*$^{-/-}$ mice were described previously[52]. The *Nox4*$^{-/-}$ mice were genotyped using standard PCR of tail DNA. All animal experimental protocols were approved by the Institutional Animal Care and Use Committee (protocol #: 2013-0108; Weill Cornell Medical College, New York, New York, USA).

Infection of *Streptococcus pneumoniae*

Streptococcus pneumoniae (*S. pneumoniae*) (ATCC 6303, ATCC, Manassas, VA) was grown on 10% sheep blood agar plates (BD Biosciences) overnight or for 4–24 h in brain heart

Author Manuscript Author Manuscript Author Manuscript Author Manuscript

infusion (BHI) broth (BD Biosciences). Colony forming units (CFU) were assessed by dilution of samples in BHI and titers were determined by colony counts × dilution. WT and *Nox4*$^{-/-}$ mice (male, 8–10 weeks old) were anesthetized with isoflurane (5% for induction and 2% for maintenance) prior to intranasal instillation with 1×10^3 CFU of *S. pneumoniae* (50 μl volume in PBS). After 24 h, the mice were sacrificed. The protein expression and the levels of IL-1β, IL-18 and TNF-α in lung tissues from WT and *Nox4*$^{-/-}$ mice were measured by immunoblot analysis and ELISA. For the mortality study, WT and *Nox4*$^{-/-}$mice (male and female, 7–9 weeks old) were anesthetized with isoflurane (5% for induction and 2% for maintenance) prior to intranasal instillation with 1×10^8 CFU of *S. pneumoniae* (50 μl volume in PBS). For *S. pneumoniae* infection experiments, in order to achieve 90% power with a two-tailed significance level (P value) of 0.05, we selected a minimum of 15 mice per group.

LPS challenge

The WT and *Nox4*$^{-/-}$ mice (male, 8–10 weeks old) were injected intraperitoneally with *Escherichia coli* LPS (10 mg/kg) (L4130, Sigma-Aldrich) or PBS. After 24 h, the mice were sacrificed. The plasma levels of IL-1β, IL-18 and TNF-α from mice were measured by ELISA. The WT mice were injected intraperitoneally (i.p.) with VAS-2870 (10 mg/kg), GKT137831 (20 mg/kg) or vehicle control (DMSO) 3 h before i.p. injection of *Escherichia coli* LPS (10 mg/kg) (L4130, Sigma-Aldrich) or PBS.

Reagents and antibodies

LPS (*Escherichia coli*) (tlrl-pelps), MDP (tlrl-mdp) and flagellin (*Salmonella typhimurium*) (tlrl-stfla) was from Invivogen. ATP (A2383), nigericin (N7143), poly(dA:dT) (P0883), *A. hydrophila aerolysin* (H9395) and Glyburide (G2539) were from Sigma-Aldrich. VAS-2870 (BML-EI395-0010) and Mito-TEMPO (ALX-430-150-M005) were from Enzo Life Sciences. ML171 (4653) was from Tocris Bioscience. GKT137831 (S7171) was from Selleckchem. The following antibodies were used: Polyclonal rabbit anti-caspase-1 for mouse caspase-1 (1:1000) (SC-514, Santa Cruz Biotechnology), Polyclonal goat anti-IL-1β for mouse IL-1β (1:1000) (AF-401-NA, R&D Systems), Polyclonal rabbit anti-ASC for mouse ASC (1:1000) (ADI-905-173-100, Enzo Lifesciences), Monoclonal rabbit anti-caspase-1 for human caspase-1 (1:1000) (3866, Cell signaling), Monoclonal mouse anti-IL-1β for human IL-1β (1:1000) (MAB201, R&D Systems), Monoclonal rabbit anti-NOX4 for human NOX4 and mouse NOX4 (1:1000) (ab133303, Abcam), Monoclonal mouse anti-CPT1A for mouse CPT1A (1:1000) (ab128568, Abcam), Polyclonal rabbit anti-CPT1C for mouse CPT1C (1:1000) (ab87498, Abcam), Monoclonal rabbit anti-CD36 antibody for mouse CD36 (1:1000) (ab133625, Abcam), Polyclonal rabbit anti-ACOX1 antibody for mouse ACOX1 (1:1000) (ab59964, Abcam), Polyclonal rabbit anti-translocase of outer mitochondrial membrane 20 (TOMM20) antibody for human TOMM20 and mouse TOMM20 (1:1000) (SC-11415, Santa Cruz Biotechnology), Monoclonal mouse anti-β-actin (1:5000) (A5316, Sigma-Aldrich).

Preparation of Bovine Serum Albumin (BSA)-Conjugated Palmitate

Sodium palmitate (P9767, Sigma-Aldrich) or stearic acid (S4751, Sigma-Aldrich) was conjugated with fatty acid-free BSA (03117405001, Roche) at a 6:1 molar ratio according to

Author Manuscript Author Manuscript Author Manuscript Author Manuscript

the manufacturer's instructions (Seahorse Biosciences). BMDMs were treated with palmitate-BSA (500 μM, 2 h), stearic acid (500 μM, 2 h) or BSA as control after LPS incubation.

Cell culture

BMDMs were prepared as described[1]. Bone marrow collected from WT and *Nox4*$^{-/-}$ mice (male, 8–10 weeks old) femurs and tibias was plated on sterile petri dishes and incubated for 7 d in DMEM media (Invitrogen) containing 10% (vol/vol) heat-inactivated FBS, 100 units/ml penicillin, 100 mg/ml streptomycin, and 25% (vol/vol) conditioned medium from mouse L929 fibroblasts (CCL-1™, ATCC). WT and *Nox4*$^{-/-}$ BMDMs (5×10^6 cells in 100 mm cell culture dish) were incubated with LPS (500 ng/ml, 4 h) and then were treated with NLRP3 inflammasome activators as described (nigericin (6.7 μM, 1 h), ATP (2 mM or 5 mM, 30 min), silica (200 ng/ml, 16 h), MDP (200 ng/ml, 16 h), flagellin (200 ng/ml, 16 h) or *A. hydrophila aerolysin* (10 ng/ml, 0.5 h or 1 h)). Mice were injected with thioglycollate broth medium (1.0 ml, i.p.). After 4 d, peritoneal cells were collected from WT and *Nox4*$^{-/-}$mice with cold PBS. Cells (1×10^6 cells in 6-well cell culture plates) were incubated for 2 h with DMEM medium containing 10% (vol/vol) heat-inactivated FBS, penicillin and streptomycin. Non-adherent cells are removed by gently washing with PBS. After cells were cultured for overnight, cells were incubated for 4 h with LPS and then were treated with NLRP3 inflammasome activators as described. The cell supernatants and cell lysates were collected and analyzed for the levels of IL-1β, IL-18 and TNF-α by ELISA. WT and *Nox4*$^{-/-}$ BMDMs were treated with medium containing KCl (100 mM, 1 h) for high extracellular [K^+] before LPS and nigericin stimulation. WT BMDMs were treated with Mito-TEMPO (100 μM, 1 h) for inhibition of mtROS production before nigericin treatment after LPS stimulation. Primary BMDMs were not tested for mycoplasma.

Primary human macrophages

Primary human peripheral blood mononuclear cells (PBMCs) were isolated in healthy donors using Ficoll-Paque™. We confirmed consent was obtained from all human subjects. Primary human monocytes were isolated from PBMCs using Monocyte Isolation Kit II (130-091–153, Miltenyi Biotec) according to the manufacturer's instructions. Primary human monocytes were differentiated to macrophages for 7 d in RPMI 1640 media (Invitrogen) containing 10% (vol/vol) heat-inactivated FBS, 100 units/ml penicillin, 100 mg/ml streptomycin, and 5 ng/ml M-CSF (216-MC-025, R&D Systems). Primary human macrophages (1×10^6 cells in 6-well cell culture plates) were incubated for 4 h with LPS (500 ng/ml) and then were treated with NLRP3 inflammasome activators as described (nigericin (6.7 μM, 1 h) or ATP (5 mM, 30 min)). All analysis of human subjects was conducted according to the guidelines of the Weill Cornell Medical College Institutional Review Board (IRB) approval (protocol #: 1405015116A003; Weill Cornell Medical College, New York, New York, USA).

Immunoblot analysis

WT and *Nox4*$^{-/-}$ BMDMs, peritoneal macrophages or lung tissues were harvested and lysed in 2 × SDS loading buffer, NP40 Cell Lysis Buffer (FNN0021, Invitrogen) or Tissue Extraction Reagent I (FNN0071, Invitrogen) and then briefly sonicated. Lysates were

Author Manuscript Author Manuscript Author Manuscript Author Manuscript

centrifuged at 15,300 g for 10 min at 4 °C, and the supernatants were obtained. The protein concentrations of the supernatants were determined using the Bradford assay (500-0006, Bio-Rad Laboratories). Proteins were electrophoresed on NuPAGE 4−12% Bis-Tris gels (Invitrogen) and transferred to Protran nitrocellulose membranes (10600001, GE Healthcare Life science). Membranes were blocked in 5% (wt/vol) bovine serum albumin (BSA) (9048-46-8, Santa Cruz Biotechnology) in TBS-T (TBS (170–6435, Bio-Rad Laboratories) and 1% (vol/vol) Tween-20 (170–6531, Bio-Rad Laboratories)) for 30 min at room temperature. Membranes were incubated with primary antibody diluted in 1% (wt/vol) BSA in TBS-T at 4 °C and then with the horseradish peroxidase (HRP)-conjugated secondary antibody (goat anti-rabbit IgG-HRP (SC-2004) (1:2500), goat anti-mouse IgG-HRP (SC-2005) (1:2500), goat anti-rabbit IgG-HRP (SC-2004) (1:2500) from Santa Cruz Biotechnology) diluted in TBS-T for 30 min at room temperature. The immunoreactive bands were detected by the SuperSignal West Pico Chemiluminescent Substrate (34078, Thermo Scientific). Mitochondrial fractions were isolated from WT and *Nox4*$^{-/-}$ BMDMs using a mitochondria/cytosol fraction kit (K265-25, Biovision) according to the manufacturer's instructions.

ASC oligomerization and ASC speck formation

WT and *Nox4*$^{-/-}$ BMDMs (5×10^6 cells in 100 mm cell culture dish) were harvested and lysed in 500 μl of lysis buffer (20 mM HEPES–KOH, pH 7.5, 150 mM KCl, 1% NP-40) as described previously[29,30]. Lysates were centrifuged at 330 × g for 10 min at 4 °C. The pellets were washed in 1 ml of PBS and resuspended in 500 μl of PBS. 2 mM disuccinimydyl suberate (DSS) was added to the resuspended pellets, which were incubated for 30 min with rotation at room temperature. Samples were then centrifuged at 330 × g for 10 min at 4 °C. The supernatant was removed, and the cross-linked pellets were resuspended in 50 μl of Laemmli sample buffer. Samples were analyzed by immunoblot analysis using polyclonal ASC antibody (ADI-905-173-100, Enzo Lifesciences). WT and *Nox4*$^{-/-}$BMDMs were seeded on chamber slides. After stimulation, cells were fixed with 4% paraformaldehyde and then incubated with polyclonal ASC antibody (ADI-905-173-100, Enzo Lifesciences) for 16 h followed by DAPI (P36962, ThermoFisher Scientific) staining as described previously[29,30]. ASC specks were analyzed by Zeiss LSM880 laser scanning confocal microscope and quantified using ImageJ software. The graph represents the quantification of cells with specks in five distinct areas.

Cytokine analysis

Supernatants from WT and *Nox4*$^{-/-}$ BMDMs or peritoneal macrophages and plasma or lung tissues from WT and *Nox4*$^{-/-}$ mice were measured for mouse IL-1β (MLB00C, R&D systems), mouse IL-18 (7625, R&D systems), mouse TNF-α (MTA00B, R&D systems) according to the manufacturer's instructions. Supernatants from primary human macrophages were measured for human IL-1β (DLB50, R&D systems), human IL-18 (7620, R&D systems) and human TNF-α (DTA00C, R&D systems) according to the manufacturer's instructions.

Author Manuscript Author Manuscript Author Manuscript Author Manuscript

Quantitative real-time PCR

Total RNA was isolated from WT and *Nox4*$^{-/-}$ BMDMs or lung tissues using the TRIzol reagent (15596-018, Invitrogen) according to the manufacturer's instructions. For quantitative RT-PCR, cDNA was synthesized from 4 μg of total RNA using random hexamers and SuperScript Reverse Transcriptase II® (18064-014, Invitrogen) according to the manufacturer's instructions. A 10 μl mixture containing the diluted cDNA and a set of gene-specific primers was mixed with 10 μl of 2 × SYBR Green PCR Master Mix (4309155, Applied Biosystems) and then subjected to RT–PCR quantification using the ABI PRISM 7500 real-time PCR system (Applied Biosystems). The following primers were used: mouse *Nox1* forward, 5'-TGAACAACAGCACTCACCAATGCC-3' and reverse, 5'-TCATTG TCCCACATTGGTCTCCCA-3'; mouse *Nox2* forward, 5'-CCCTTTGGTACAGCCAGT GAAGAT-3' and reverse, 5'-CAATCCCGGCTCCCACTAACATCA-3'; mouse *Nox3* forward, 5'-TTGTGGCACACTTGTTCAACCTGG-3' and reverse, 5'-TCACACGCA TACAAGACCACAGGA-3'; mouse *Nox4* forward, 5'-TCATGGATCTTTGCCTCG AGGGTT-3' and reverse, 5'-AGTGACTCCTCAAATGGGCTTCCA-3'; mouse *Duox1* forward, 5'-CACCATTGGGACCCTTTGCTGTTT-3' and reverse, 5'-AGCCTTTCATGA AGACCACCAGGA-3'; mouse *Duox2* forward, 5'-AACCACCTATCTGGGCATCAT CCT-3' and reverse, 5'-AGCTGCCATGGATGATGATCTGGA-3′; mouse *Cpt1a* forward, 5'-GGTCTTCTCGGGTCGAAAGC-3' and reverse, 5'-TCCTCCCACCAGTCACTCAC-3'; mouse *Gapdh* forward, 5'-GGTGAAGGTCGGTGTGAACGGA-3' and reverse, 5'-CCAAAGTTGTCATGGATGACCTTGG-3'.

Transduction of shRNA or gRNA/Cas9 plasmid

For stable knockdown of human *NOX4*, two independent NOX4-targeted gRNAs (S19475 and S19481, GeneScript) were used. Primary human macrophages (2×10^5 cells in 6-well cell culture plates) were seeded and were transduced with gRNA/Cas9 lentiviral plasmids against human *NOX4* or pLentiCRISPR v2 for control. For stable knockdown of mouse *Cpt1a*, two independent *Cpt1a*-targeted gRNAs (C91581 and C92251, GeneScript) were used. WT BMDMs (5×10^5 cells in 6-well cell culture plates) were seeded and were transduced with gRNA/Cas9 lentiviral plasmids against mouse *Cpt1a* or pLentiCRISPR v2 for control. For stable knockdown of mouse *Cpt1a*, two independent small hairpin RNA (TRCN0000305935 and TRCN0000110598, Sigma-Aldrich) were used. WT peritoneal macrophages (5×10^5 cells in 6-well cell culture plates) were seeded and were transduced with shRNA lentiviral constructs against mouse *Cpt1a* or non-target shRNA (SHC016, Sigma-Aldrich) for control. For stable over-expression of mouse *Nox4*, lenti ORF clone of *Nox4* (Myc-DDK-tagged) (MR227192, Origene) was used. For stable over-expression of mouse CPT1A, lenti ORF clone of *Cpt1a* (Myc-DDK-tagged) (MR210568L1, Origene) was used. For stable over-expression of mouse NLRP3, lenti ORF clone of *Nlrp3* (Myc-DDK-tagged) (MR227218, Origene) was used. For AIM2 inflammasome activation, LPS-primed WT and *Nox4*$^{-/-}$ BMDMs or peritoneal macrophages were transfected with poly(dA:dT) (1 μg/ml) (Sigma-Aldrich) using Lipofectamine® with Plus reagent (15338-100, Invitrogen) according to the manufacturer's instructions.

Author Manuscript Author Manuscript Author Manuscript Author Manuscript

Mitochondrial ROS production assay

Mitochondrial ROS were measured by MitoSOX (M36008, Invitrogen) staining. WT and *Nox4*$^{-/-}$ BMDMs or peritoneal macrophages were incubated with mitochondrial superoxide-specific stain MitoSOX (5 μM) for 15 min at 37 °C. WT and *Nox4*$^{-/-}$ BMDMs or peritoneal macrophages were washed with PBS, treated with trypsin and resuspended in PBS containing 1% (vol/vol) heat-inactivated FBS. Data were acquired with a BD Accuri™ C6 Cytometer (BD Biosciences) and were analyzed with FlowJo analytical software (TreeStar).

Metabolomic analysis

WT BMDMs stimulated with LPS and ATP. All samples (n = 6 per group) were harvested with PBS. All samples were inventoried and immediately stored at −80 °C. At the time of analysis, samples were extracted and prepared for analysis using a standard solvent extraction method (Metabolon). The extracted samples were split into equal parts for analysis on the GC/MS and LC/MS/MS platform, according to the manufacturer's instructions (Metabolon).

Fatty acid assay

Free fatty acid levels in WT and *Nox4*$^{-/-}$ BMDMs or peritoneal macrophages were measured using the Free Fatty Acid Quantification Colorimetric/Fluorometric Kit (K612-100, Biovision) according to the manufacturer's instructions. Intracellular acetyl-CoA levels in WT and *Nox4*$^{-/-}$ BMDMs or peritoneal macrophages were measured by PicoProbe™ Acetyl-CoA Fluorometric Assay Kit (K317-100, Biovision) according to the manufacturer's instructions.

Fatty acid oxidation assay

For the fatty acid oxidation assay, WT and *Nox4*$^{-/-}$ BMDMs (5×10^4 cells/well) were plated on XF96 cell culture microplates (101085–004, Seahorse Bioscience). The OCR as parameters of mitochondrial fatty acid oxidation was measured on a Seahorse XF96 bioanalyzer, using the XF Palmitate-BSA FAO Substrate (102720-100, Seahorse Bioscience) and Mito Stress Test Kit (103015-100, Seahorse Bioscience) according to the manufacturer's instructions. The OCR for oxidation of palmitate-BSA was measured in WT and *Nox4*$^{-/-}$ BMDMs treated with palmitate-BSA (180 μM), etomoxir (40 μM) and oligomycin (1 μM).

Glycolytic function assay

For the glycolytic function assay, WT and *Nox4*$^{-/-}$ BMDMs (5×10^4 cells/well) were plated on XF96 cell culture microplates (101085-004, Seahorse Bioscience). The ECAR as parameters of glycolytic flux was measured on a Seahorse XF96 bioanalyzer, using the XF Glycolysis Stress Test Kit (102194–100, Seahorse Bioscience) according to the manufacturer's instructions. The ECAR was measured in WT and *Nox4*$^{-/-}$ BMDMs treated with glucose (10 mM), oligomycin (2 μM) and 2DG (10 mM).

Author Manuscript Author Manuscript Author Manuscript Author Manuscript

Statistical analysis

All statistical tests of data were analyzed by Student's two-tailed t-test for comparison of two groups, analysis of variance (ANOVA) (with post hoc comparisons using Dunnett's test) using a statistical software package (GraphPad Prism version 4.0) for comparison of multiple groups. Survival analyses were performed using a log-rank test using a statistical software package (GraphPad Prism version 4.0). Sample size (number of mice) was determined on the basis of our previous studies[7,53]. *P* values of less than 0.05 were considered statistically significant. All data are mean ± s.d., combined from three independent experiments.

Supplementary Material

Refer to Web version on PubMed Central for supplementary material.

Acknowledgments

This work was supported by National Institutes of Health (P01 HL108801, R01 HL079904, R01 HL055330 to A.M.K.C.). We thank E. Finkelsztein for technical assistance.

REFERENCES

1. Sutterwala FS, et al. Critical role for NALP3/CIAS1/Cryopyrin in innate and adaptive immunity through its regulation of caspase-1. Immunity. 2006; 24:317–327. [PubMed: 16546100]
2. Franchi L, Eigenbrod T, Munoz-Planillo R, Nunez G. The inflammasome: a caspase-1-activation platform that regulates immune responses and disease pathogenesis. Nat Immunol. 2009; 10:241–247. [PubMed: 19221555]
3. Hotamisligil GS. Inflammation and metabolic disorders. Nature. 2006; 444:860–867. [PubMed: 17167474]
4. Wen H, et al. Fatty acid-induced NLRP3-ASC inflammasome activation interferes with insulin signaling. Nat Immunol. 2011; 12:408–415. [PubMed: 21478880]
5. Youm YH, et al. The ketone metabolite β-hydroxybutyrate blocks NLRP3 inflammasome-mediated inflammatory disease. Nat Med. 2015; 21:263–269. [PubMed: 25686106]
6. Moon JS, et al. mTORC1-induced HK1-dependent glycolysis regulates NLRP3 inflammasome activation. Cell Rep. 2015; 12:102–115. [PubMed: 26119735]
7. Moon JS, et al. UCP2-induced fatty acid synthase promotes NLRP3 inflammasome activation during sepsis. J Clin Invest. 2015; 125:665–680. [PubMed: 25574840]
8. Vandanmagsar B, et al. The NLRP3 inflammasome instigates obesity-induced inflammation and insulin resistance. Nat. Med. 2011; 17:179–188. [PubMed: 21217695]
9. Carracedo A, Cantley LC, Pandolfi PP. Cancer metabolism: fatty acid oxidation in the limelight. Nat Rev Cancer. 2013; 13:227–232. [PubMed: 23446547]
10. Currie E, et al. Cellular fatty acid metabolism and cancer. Cell Metab. 2013; 18:153–161. [PubMed: 23791484]
11. Rasmussen BB, et al. Malonyl coenzyme A and the regulation of functional carnitine palmitoyltransferase-1 activity and fat oxidation in human skeletal muscle. J Clin Invest. 2002; 110:1687–1693. [PubMed: 12464674]
12. McGarry JD, Mills SE, Long CS, Foster DW. Observations on the affinity for carnitine, and malonyl-CoA sensitivity, of carnitine palmitoyltransferase I in animal and human tissues. Demonstration of the presence of malonyl-CoA in non-hepatic tissues of the rat. Biochem J. 1983; 214:21–28. [PubMed: 6615466]

Author Manuscript Author Manuscript Author Manuscript Author Manuscript

13. Drummond GR, Selemidis S, Griendling KK, Sobey CG. Combating oxidative stress in vascular disease: NADPH oxidases as therapeutic targets. Nat Rev Drug Discov. 2011; 10:453–471. [PubMed: 21629295]
14. Hecker L, et al. NADPH oxidase-4 mediates myofibroblast activation and fibrogenic responses to lung injury. Nat Med. 2009; 15:1077–1081. [PubMed: 19701206]
15. Weyemi U, et al. ROS-generating NADPH oxidase NOX4 is a critical mediator in oncogenic H-Ras-induced DNA damage and subsequent senescence. Oncogene. 2012; 31:1117–1129. [PubMed: 21841825]
16. Geiszt M, Kopp JB, Varnai P, Leto TL. Identification of renox, an NAD(P)H oxidase in kidney. Proc. Natl Acad. Sci. USA. 2000; 97:8010–8014. [PubMed: 10869423]
17. Goettsch C, et al. NADPH oxidase 4 limits bone mass by promoting osteoclastogenesis. J Clin Invest. 2013; 123:4731–4718. [PubMed: 24216508]
18. Cheng G, Cao Z, Xu X, van Meir EG, Lambeth JD. Homologs of gp91phox: cloning and tissue expression of Nox3, Nox4, and Nox5. Gene. 2001; 269:131–140. [PubMed: 11376945]
19. Block K, Gorin Y, Abboud HE. Subcellular localization of Nox4 and regulation in diabetes. Proc Natl Acad Sci U S A. 2009; 106:14385–14390. [PubMed: 19706525]
20. Kuroda J, et al. NADPH oxidase 4 (Nox4) is a major source of oxidative stress in the failing heart. Proc Natl Acad Sci U S A. 2010; 107:15565–15570. [PubMed: 20713697]
21. Gorin Y, et al. Nox4 NAD(P)H oxidase mediates hypertrophy and fibronectin expression in the diabetic kidney. J Biol Chem. 2005; 280:39616–39626. [PubMed: 16135519]
22. Witzenrath M, et al. The NLRP3 inflammasome is differentially activated by pneumolysin variants and contributes to host defense in pneumococcal pneumonia. J. Immunol. 2011; 187:434–440. [PubMed: 21646297]
23. McNeela EA, et al. Pneumolysin activates the NLRP3 inflammasome and promotes proinflammatory cytokines independently of TLR4. PLoS Pathog. 2010; 6:e1001191. [PubMed: 21085613]
24. Assaily W, et al. ROS-mediated p53 induction of Lpin1 regulates fatty acid oxidation in response to nutritional stress. Mol Cell. 2011; 44:491–501. [PubMed: 22055193]
25. Susztak K, Ciccone E, McCue P, Sharma K, Bottinger EP. Multiple metabolic hits converge on CD36 as novel mediator of tubular epithelial apoptosis in diabetic nephropathy. PLoS Med. 2005; 2:e45. [PubMed: 15737001]
26. Huynh FK, Green MF, Koves TR, Hirschey MD. Measurement of fatty acid oxidation rates in animal tissues and cell lines. Methods Enzymol. 2014; 542:391–405. [PubMed: 24862277]
27. Mensink RP. Effects of stearic acid on plasma lipid and lipoproteins in humans. Lipids. 2005; 40:1201–1205. [PubMed: 16477803]
28. Pandolfi PP, et al. Targeted disruption of the housekeeping gene encoding glucose 6-phosphate dehydrogenase (G6PD): G6PD is dispensable for pentose synthesis but essential for defense against oxidative stress. EMBO J. 1995; 14:5209–5215. [PubMed: 7489710]
29. Lu A, et al. Unified polymerization mechanism for the assembly of ASC-dependent inflammasomes. Cell. 2014; 156:1193–1206. [PubMed: 24630722]
30. Yu JW, et al. Cryopyrin and pyrin activate caspase-1, but not NF-κB, via ASC oligomerization. Cell Death Differ. 2006; 13:236–249. [PubMed: 16037825]
31. McGarry JD, Brown NF. The mitochondrial carnitine palmitoyltransferase system. From concept to molecular analysis. Eur J Biochem. 1997; 244:1–14. [PubMed: 9063439]
32. Varanasi U, et al. Isolation of the human peroxisomal acyl-CoA oxidase gene: organization, promoter analysis, and chromosomal localization. Proc Natl Acad Sci U S A. 1994; 91:3107–3111. [PubMed: 8159712]
33. Muñoz-Planillo R, et al. K^+ efflux is the common trigger of NLRP3 inflammasome activation by bacterial toxins and particulate matter. Immunity. 2013; 38:1142–1153. [PubMed: 23809161]
34. Ashcroft FM, et al. ATP-sensitive potassium channelopathies: focus on insulin secretion. J. Clin. Invest. 2005; 115:2047–2058. [PubMed: 16075046]
35. Trnka J, Blaikie FH, Logan A, Smith RA, Murphy MP. Antioxidant properties of MitoTEMPOL and its hydroxylamine. Free Radic Res. 2009; 43:4–12. [PubMed: 19058062]

Author Manuscript Author Manuscript Author Manuscript Author Manuscript

36. Tran M, et al. PGC-1α promotes recovery after acute kidney injury during systemic inflammation in mice. J Clin Invest. 2011; 121:4003–4014. [PubMed: 21881206]
37. Tutwiler GF, Brentzel HJ, Kiorpes TC. Inhibition of mitochondrial carnitine palmitoyl transferase A in vivo with methyl 2-tetradecylglycidate (methyl palmoxirate) and its relationship to ketonemia and glycemia. Proc. Soc. Exp. Biol. Med. 1985; 178:288–296. [PubMed: 3969383]
38. Aoyama T, et al. Nicotinamide adenine dinucleotide phosphate oxidase in experimental liver fibrosis: GKT137831 as a novel potential therapeutic agent. Hepatology. 2012; 56:2316–2327. [PubMed: 22806357]
39. Boden G, Shulman GI. Free fatty acids in obesity and type 2 diabetes: defining their role in the development of insulin resistance and beta-cell dysfunction. Eur J Clin Invest. 2002; 32:14–23. [PubMed: 12028371]
40. Karpe F, Dickmann JR, Frayn KN. Fatty acids, obesity, and insulin resistance: time for a reevaluation. Diabetes. 2011; 60:2441–2449. [PubMed: 21948998]
41. Choi AM, Nakahira K. Dampening insulin signaling by an NLRP3 'meta-flammasome'. Nat Immunol. 2011; 5:379–380.
42. Mihaylova MM, Shaw RJ. The AMPK signalling pathway coordinates cell growth, autophagy and metabolism. Nat Cell Biol. 2011; 13:1016–1023. [PubMed: 21892142]
43. Wanders RJ, et al. The enzymology of mitochondrial fatty acid beta-oxidation and its application to follow-up analysis of positive neonatal screening results. J Inherit Metab Dis. 2010; 33:479–494. [PubMed: 20490924]
44. Herrero L, et al. Alteration of the malonyl-CoA/carnitine palmitoyltransferase I interaction in the beta-cell impairs glucose-induced insulin secretion. Diabetes. 2005; 54:462–471. [PubMed: 15677504]
45. Nolan CJ, et al. Fatty acid signaling in the beta-cell and insulin secretion. Diabetes. 2006; 55:S16–S23. [PubMed: 17130640]
46. Roden M. Mechanisms of disease: hepatic steatosis in type 2 diabetes-pathogenesis and clinical relevance. Nat. Clin. Pract. Endocrinol. Metab. 2006; 2:335–348. [PubMed: 16932311]
47. Brookheart RT, Michel CI, Schaffer JE. As a matter of fat. Cell Metab. 2009; 10:9–12. [PubMed: 19583949]
48. Lagathu C, et al. Long-term treatment with interleukin-1beta induces insulin resistance in murine and human adipocytes. Diabetologia. 2006; 49:2162–2173. [PubMed: 16865359]
49. Larsen CM, et al. Interleukin-1-receptor antagonist in type 2 diabetes mellitus. N. Engl. J. Med. 2007; 356:1517–1526. [PubMed: 17429083]
50. Mandrup-Poulsen T, Pickersgill L, Donath MY. Blockade of interleukin 1 in type 1 diabetes mellitus. Nat. Rev. Endocrinol. 2010; 6:158–166. [PubMed: 20173777]
51. Coll RC, et al. A small-molecule inhibitor of the NLRP3 inflammasome for the treatment of inflammatory diseases. Nat Med. 2015; 21:248–255. [PubMed: 25686105]

References

52. Carnesecchi S, et al. A key role for NOX4 in epithelial cell death during development of lung fibrosis. Antioxid Redox Signal. 2011; 15:607–619. [PubMed: 21391892]
53. Nakahira K, et al. Autophagy proteins regulate innate immune responses by inhibiting the release of mitochondrial DNA mediated by the NALP3 inflammasome. Nat Immunol. 2011; 12:222–230. [PubMed: 21151103]

Author Manuscript Author Manuscript Author Manuscript Author Manuscript

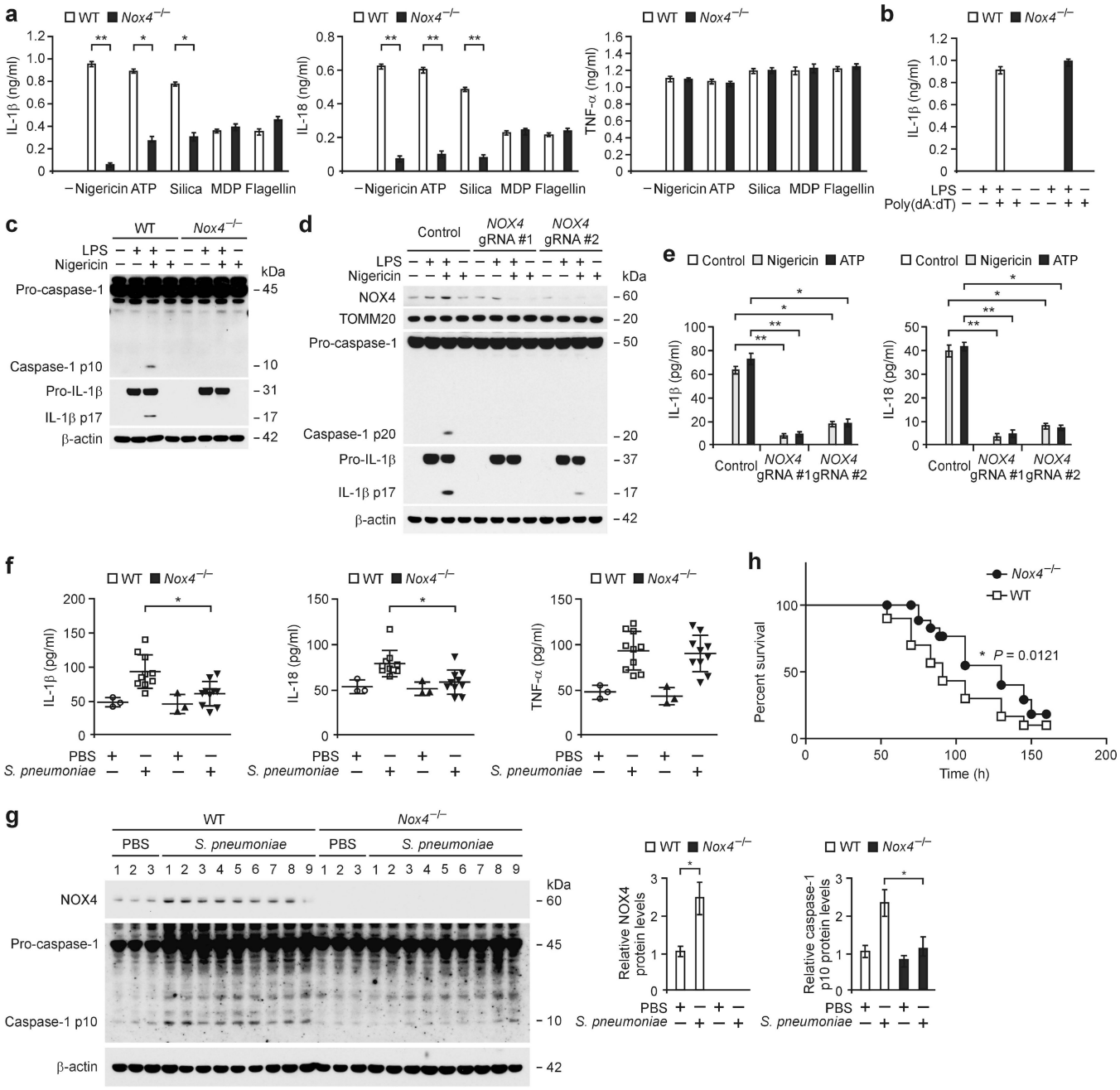

Figure 1.

Deficiency of NOX4 suppresses NLRP3 inflammasome activation. (**a,b**) The results of ELISA from LPS-primed WT and *Nox4*$^{-/-}$ BMDMs for (**a**) IL-1β, IL-18 and TNF-α after stimulation with nigericin, ATP, silica, MDP or flagellin and (**b**) for IL-1β after stimulation with poly(dA:dT). (**c**) Immunoblot analysis for caspase-1 and IL-1β from LPS-primed WT and *Nox4*$^{-/-}$ BMDMs stimulated with nigericin. (**d**) Immunoblot analysis for NOX4 in mitochondrial fraction, caspase-1 and IL-1β in cytosolic fraction and (**e**) ELISA for IL-1β and IL-18 from primary human macrophages transduced with lentivirus expressing two independent *NOX4*-targeted gRNAs (*NOX4* gRNA #1 and *NOX4* gRNA #2) and control

Author Manuscript Author Manuscript Author Manuscript Author Manuscript

plasmid (Control), and stimulated with LPS and nigericin or ATP. (**f**) ELISA for IL-1β, IL-18 and TNF-α and (**g**) Immunoblot analysis for NOX4 and caspase-1 in lung tissues (100 μg) from WT and *Nox4*$^{-/-}$ mice after infection of *S. pneumoniae* or PBS for 24 h (PBS, n = 3 and *S. pneumoniae,* n = 10). (**h**) Survival curve of *S. pneumoniae* infection was determined in WT and *Nox4*$^{-/-}$ mice (WT, n = 30 and *Nox4*$^{-/-}$, n = 30, P = 0.0121 by log-rank test). TOMM20 and β-actin served as the standard. Data are derived from n = 6 (**a**); n = 3 (**b**); or n = 6 (**c**) mice and n = 3 (**d**) human subjects. All data are mean ± s.d., $^{**}P < 0.01$ by ANOVA. $^{*}P < 0.05$ by ANOVA. Data are representative of three independent experiments and each carried out in triplicate.

Author Manuscript Author Manuscript Author Manuscript Author Manuscript

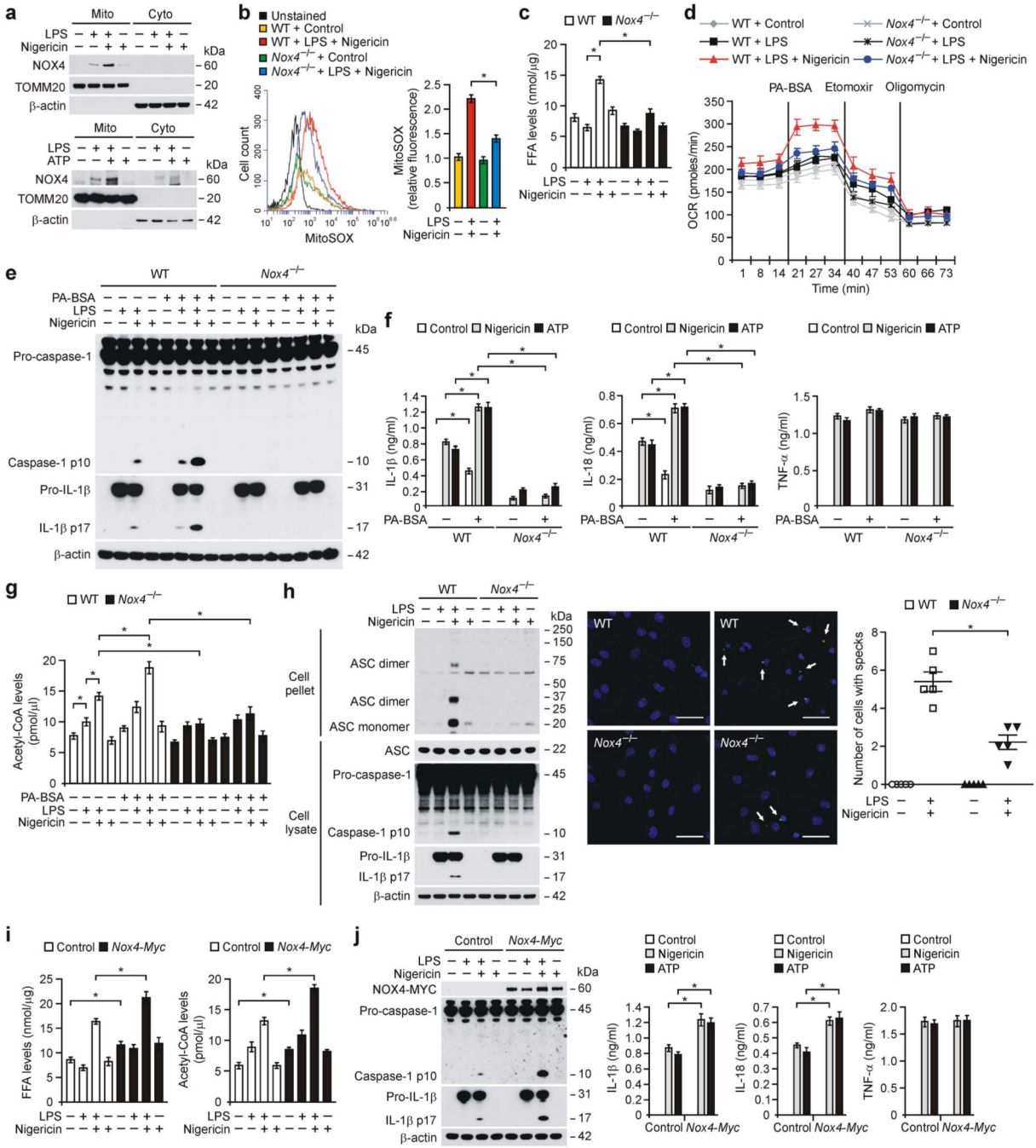

Figure 2.

NOX4 regulates FAO during NLRP3 inflammasome activation. (**a**) Immunoblot analysis for NOX4 in mitochondrial (Mito) and cytosolic (Cyto) fractions from LPS-primed WT BMDMs stimulated with nigericin or ATP. (**b**) Flow cytometry analysis of WT and *Nox4*$^{-/-}$ BMDMs stained with MitoSOX and then treated with nigericin after LPS. (**c**) FFA levels and (**d**) OCR for oxidation of palmitate-BSA (PA-BSA) from WT and *Nox4*$^{-/-}$ BMDMs stimulated with LPS and nigericin. (**e**) Immunoblot analysis for caspase-1 and IL-1β and (**f**) ELISA for IL-1β, IL-18 and TNF-α and (**g**) Acetyl-CoA levels from LPS-primed WT and

Author Manuscript Author Manuscript Author Manuscript Author Manuscript

Nox4$^{-/-}$ BMDMs incubated with PA–BSA, nigericin or ATP. (**h**) Immunoblot analysis (left) for DSS–cross-linked ASC, ASC, caspase-1 and IL-1β from WT and *Nox4*$^{-/-}$ BMDMs stimulated with LPS and nigericin. Representative immunofluorescence images ($n = 5$ per group) (right) of ASC speck formation (white arrows) in WT and *Nox4*$^{-/-}$ BMDMs stimulated with LPS and nigericin (right) or control (left). Scale bars, 20 μm. (**i**) FFA and acetyl-CoA levels and (**j**) Immunoblot analysis for NOX4, caspase-1 and IL-1β and ELISA for IL-1β, IL-18 and TNF-α in control and *Nox4* over-expressed peritoneal macrophages stimulated with LPS and nigericin or ATP. All data are mean ± s.d., $*P < 0.05$ by ANOVA. Data are derived from $n = 5$ (**a**); $n = 3$ (**b**); $n = 5$ (**c**); $n = 6$ (**d–f**); $n = 5$ (**g**); $n = 6$ (**h**) or $n = 10$ (**i,j**) mice with three independent experiments.

Author Manuscript Author Manuscript Author Manuscript Author Manuscript

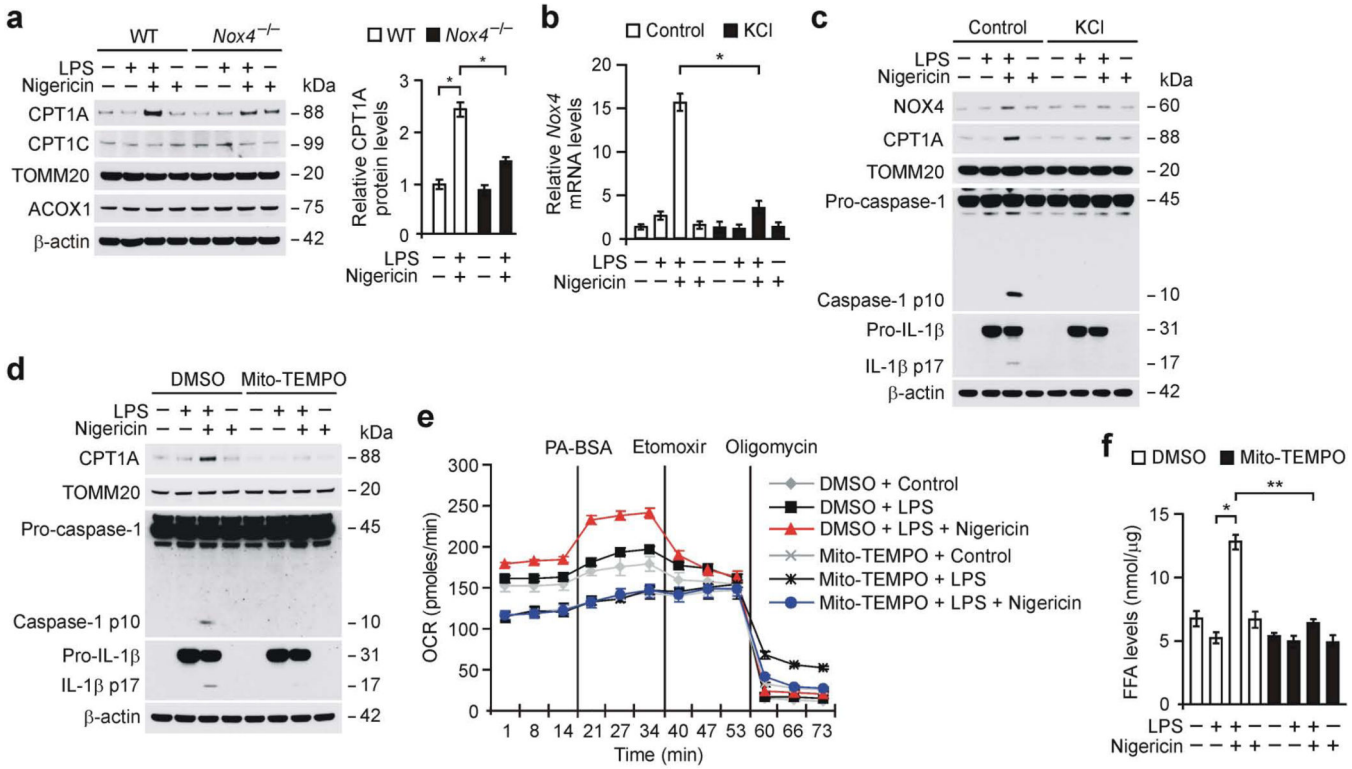

Figure 3.

NOX4 regulates CPT1A in NLRP3 inflammasome activation. (**a**) Immunoblot analysis for CPT1A and CPT1C in mitochondrial fractions and ACOX1 in cytosolic fractions from WT and *Nox4*$^{-/-}$ BMDMs stimulated with LPS and nigericin. Data are normalized to TOMM20. (**b**) Quantitative PCR analysis for *Nox4* gene expression from WT BMDMs in medium containing KCl (100 mM, 1 h) stimulated with LPS and nigericin. (**c**) Immunoblot analysis for NOX4 and CPT1A in mitochondrial fraction and caspase-1 and IL-1β in cytosolic fraction from WT BMDMs in medium containing KCl stimulated with LPS and nigericin. (**d**) Immunoblot analysis for CPT1A in mitochondrial fractions and caspase-1 and IL-1β in cytosolic fractions from WT BMDMs pre-treated with Mito-TEMPO (100 μM, 1 h) before nigericin treatment after LPS stimulation. (**e**) OCR for oxidation of palmitate-BSA was measured in WT BMDMs pre-treated with Mito-TEMPO before nigericin treatment after LPS stimulation. (**f**) Intracellular FFA levels in WT BMDMs pre-treated with Mito-TEMPO before nigericin treatment after LPS stimulation. TOMM20 and β-actin served as the standard. Data are derived from $n = 5$ (**a**); $n = 6$ (**b,c**); $n = 3$ (**d**); or $n = 5$ (**e,f**) mice. All data are mean ± s.d., $^{**}P < 0.01$ by ANOVA. $^{*}P < 0.05$ by ANOVA. Data are representative of three independent experiments and each carried out in triplicate.

Author Manuscript Author Manuscript Author Manuscript Author Manuscript

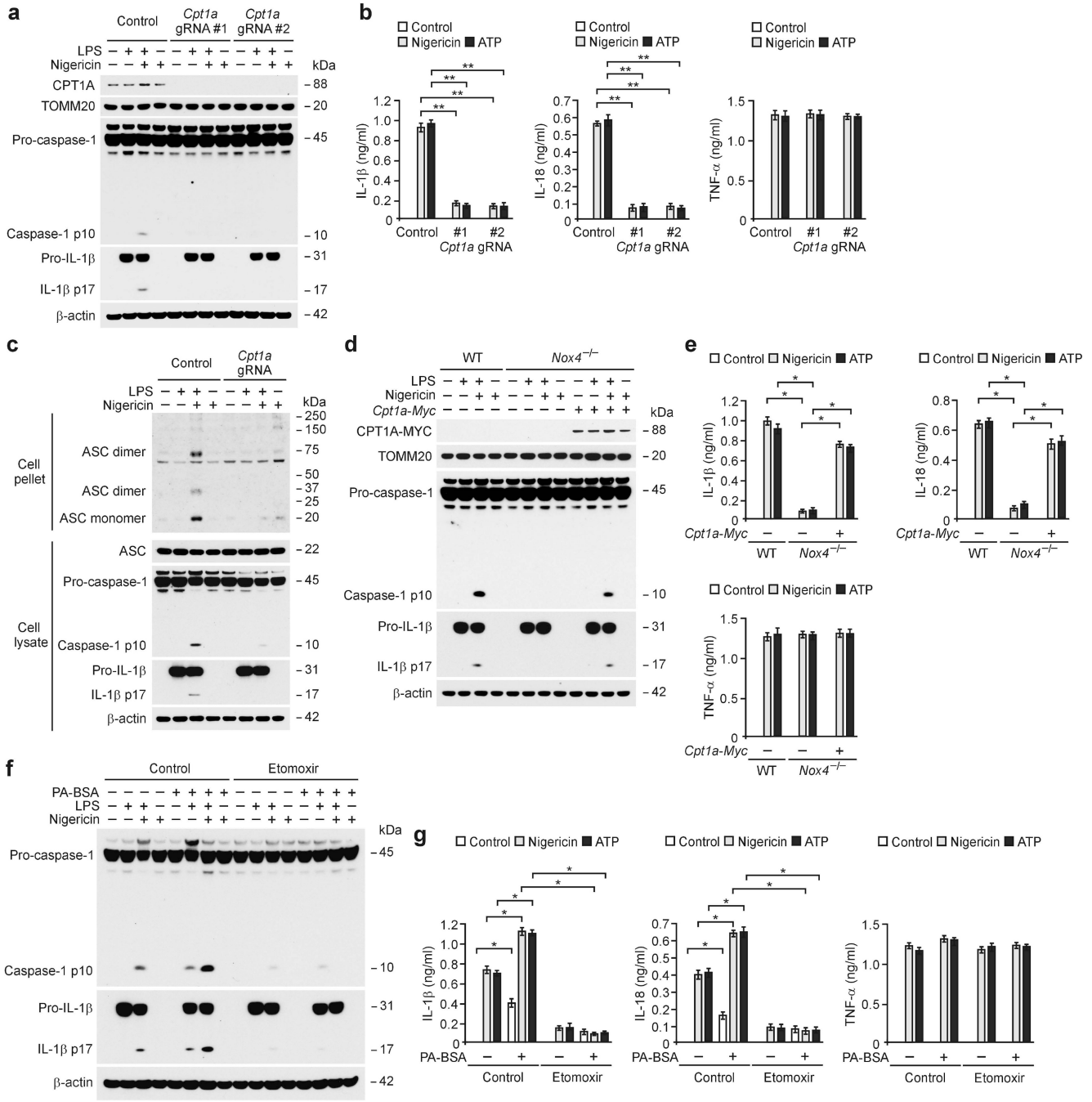

Figure 4.

Inhibition of FAO suppresses NLRP3 inflammasome activation. (**a**) Immunoblot analysis for CPT1A in mitochondrial fractions, caspase-1 and IL-1β in cytosolic fractions and (**b**) ELISA for IL-1β, IL-18 and TNF-α from WT BMDMs transduced with lentivirus expressing two independent *Cpt1a*-targeted gRNAs (*Cpt1a* gRNA#1 and gRNA#2) and control plasmid (Control), and stimulated with LPS and nigericin. (**c**) Immunoblot analysis for DSS–cross-linked ASC of cross-linked cytosolic pellets, and ASC, caspase-1 and IL-1β of cell lysates from WT BMDMs transduced with lentivirus expressing *Cpt1a*-targeted

Author Manuscript Author Manuscript Author Manuscript Author Manuscript

gRNA (*Cpt1a* gRNA) and control plasmid (Control), and stimulated with LPS and nigericin. (**d**) Immunoblot analysis for CPT1A in mitochondrial fractions, caspase-1 and IL-1β in cytosolic fractions from control and *Cpt1a* over-expressed in $Nox4^{-/-}$ BMDMs stimulated with LPS and nigericin. (**e**) ELISA for IL-1β, IL-18 and TNF-α from control and *Cpt1a* over-expressed in $Nox4^{-/-}$ BMDMs stimulated with LPS and nigericin or ATP. (**f**) Immunoblot analysis for caspase-1 and IL-1β and (**g**) ELISA for IL-1β, IL-18 and TNF-α from WT BMDMs pre-treated with etomoxir (200 μM, 1 h) or distilled water (Control), followed by incubation with palmitate-BSA (PA-BSA), nigericin or ATP after LPS stimulation. TOMM20 and β-actin served as the standard. Data are derived from $n = 6$ (**a,b**); $n = 5$ (**c**); $n = 8$ (**d,e**); or $n = 6$ (**f,g**) mice. All data are mean ± s.d., $^{**}P < 0.01$ by ANOVA. $^{*}P < 0.05$ by ANOVA. Data are representative of three independent experiments and each carried out in triplicate.

Author Manuscript Author Manuscript Author Manuscript Author Manuscript

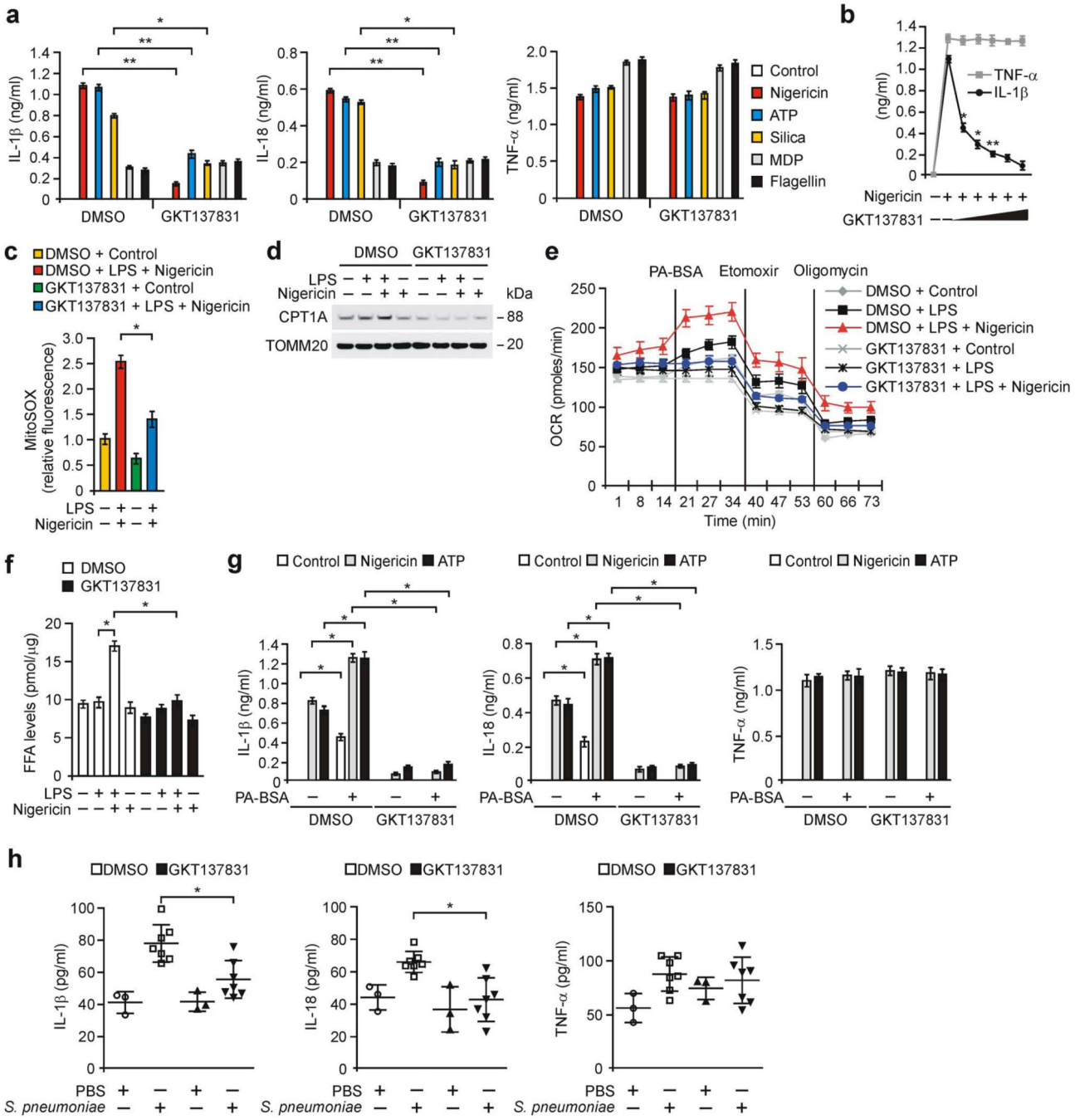

Figure 5.

GKT137831 suppresses NLRP3 inflammasome activation. (**a**) ELISA for IL-1β, IL-18 and TNF-α from WT peritoneal macrophages pre-treated with GKT137831 (20 μM, 1 h) or DMSO before LPS stimulation and followed with ATP, nigericin, silica, MDP or flagellin. (**b**) ELISA for IL-1β and TNF-α from WT peritoneal macrophages pre-treated with GKT137831 (0, 5 10, 20, 50 or 100 μM, 1 h) before LPS and nigericin. (**c**) Flow cytometry analysis of WT peritoneal macrophages stained with MitoSOX and then treated with GKT137831 or DMSO before LPS and nigericin. (**d**) Immunoblot analysis forCPT1A in

Author Manuscript Author Manuscript Author Manuscript Author Manuscript

mitochondrial fractions and (**e**) OCR for oxidation of palmitate-BSA (PA-BSA) and (**f**) FFA levels from WT BMDMs pre-treated with GKT137831 or DMSO before nigericin stimulation after LPS. TOMM20 served as the standard. (**g**) ELISA for IL-1β, IL-18 and TNF-α from WT BMDMs pre-treated with GKT137831 or DMSO, followed by incubation with PA-BSA, nigericin or ATP after LPS. (**h**) ELISA for IL-1β, IL-18 and TNF-α in lung tissues (100 μg) from WT mice after i.p. injection of GKT137831 (20 mg/kg, 3 h) or DMSO, then infection of *S. pneumoniae* or PBS for 24 h (PBS, $n = 3$ and *S. pnumoniae,* $n = 7$). Data are derived from $n = 6$ (**a,b**); $n = 5$ (**c**); $n = 3$ (**d**); $n = 5$ (**e**); or $n = 6$ (**f,g**) mice. All data are mean ± s.d., $^{**}P < 0.01$ by ANOVA. $^{*}P < 0.05$ by ANOVA. Data are representative of three independent experiments and each carried out in triplicate.

Author Manuscript
Author Manuscript
Author Manuscript
Author Manuscript

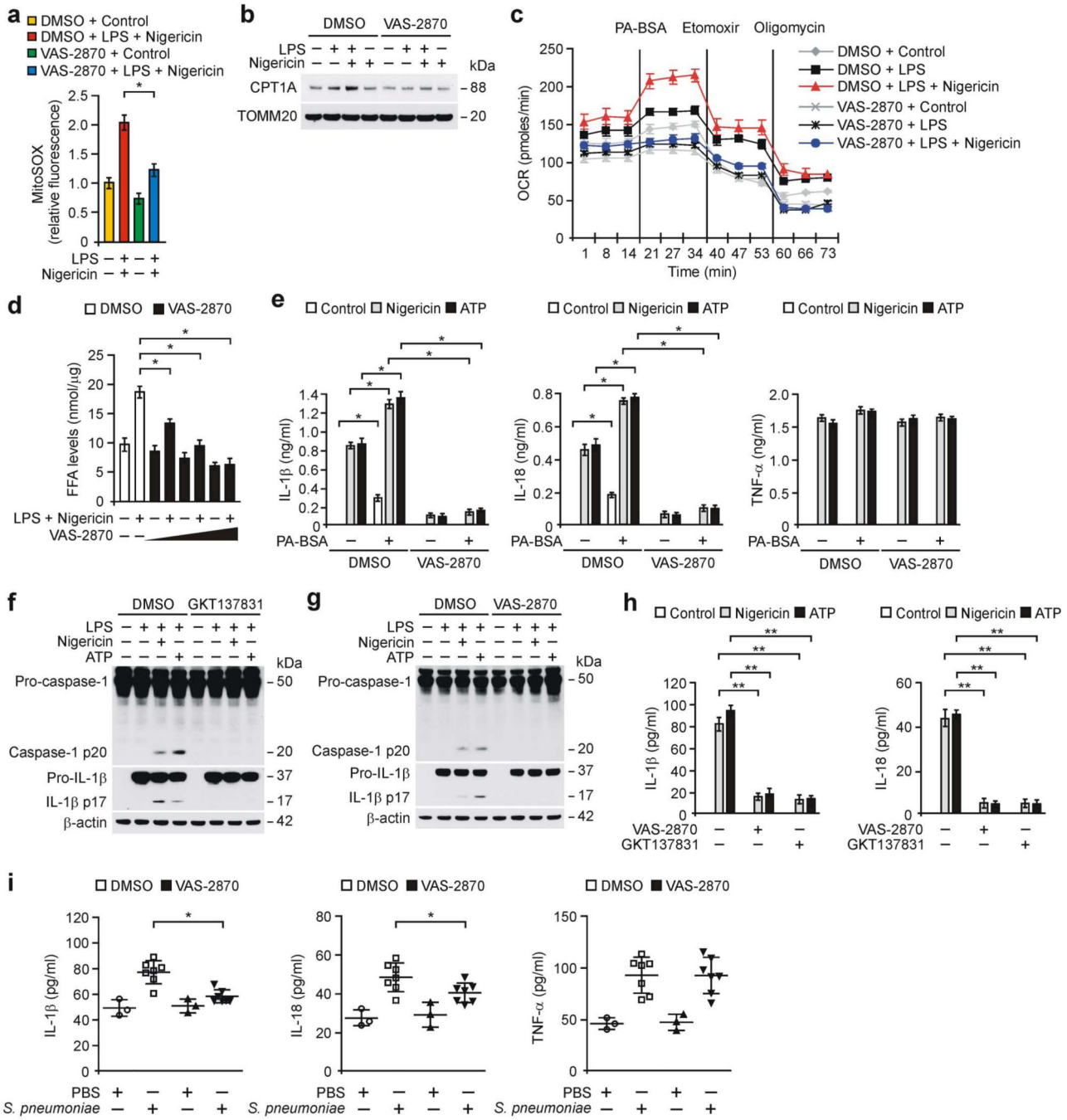

Figure 6.

Inhibition of NOX4 suppresses NLRP3 inflammasome activation. (**a**) Flow cytometry analysis of WT peritoneal macrophages stained with MitoSOX and then treated with VAS-2870 (1 μM, 1 h) or DMSO before nigericin stimulation after LPS. (**b**) Immunoblot analysis for CPT1A in mitochondrial fractions and (**c**) OCR for oxidation of palmitate-BSA (PA-BSA) from WT BMDMs pre-treated with VAS-2870 or DMSO before nigericin stimulation after LPS. (**d**) FFA levels in WT BMDMs pre-treated with VAS-2870 before nigericin stimulation after LPS. (**e**) ELISA for IL-1β, IL-18 and TNF-α from WT BMDMs

Author Manuscript Author Manuscript Author Manuscript Author Manuscript

pre-treated with VAS-2870 or DMSO, followed by incubation with PA-BSA, nigericin or ATP after LPS stimulation. (**f,g**) Immunoblot analysis for caspase-1 and IL-1β and (**h**) ELISA for IL-1β, IL-18 and TNF-α from primary human macrophages pre-treated with GKT137831 (20 μM, 1 h), VAS-2870 (2 μM, 1 h) or DMSO before nigericin or ATP stimulation after LPS. (**i**) ELISA for IL-1β, IL-18 and TNF-α in lung tissues (100 μg) from WT mice after i.p. injection of VAS-2870 (10 mg/kg, 3 h) or DMSO, then infection of *S. pneumoniae* or PBS for 24 h (PBS, $n = 3$ and *S. pnumoniae,* $n = 7$). Data are derived from $n = 5$ (**a**); $n = 3$ (**b**); n = 5 (**c,d**); $n = 6$ (**e**) mice; or $n = 3$ (**f**–**h**) human subjects. All data are mean ± s.d., $^{**}P < 0.01$ by ANOVA. $^{*}P < 0.05$ by ANOVA. Data are representative of three independent experiments and each carried out in triplicate.